Journal of Inorganic Biochemistry 197 (2019) 110701

Contents lists available at ScienceDirect

Journal of Inorganic Biochemistry

journal homepage: www.elsevier.com/locate/jinorgbio

Synthesis of a novel platinum(II) complex with 6,7-dichloro-5,8-quinolinedione and the study of its antitumor mechanism in testicular seminoma

Zitaiyu Li[a], Jun Zhou[a], Yu Gan[b], Yinghao Yin[a], Wuchao Zhang[a], Jianfu Yang[a], Yuxin Tang[c,*], Yingbo Dai[c]

[a] Department of Urology, The Third Xiangya Hospital of Central South University, Central South University, Changsha 410000, China
[b] Department of Urology, Xiangya Hospital of Central South University, Central South University, Changsha 410000, China
[c] Department of Urology, The Fifth Affiliated Hospital of Sun Yat-sen University, Sun Yat-sen University, Zhuhai 519000, China

ARTICLE INFO

Keywords:
6,7-Dichloro-5,8-quinolinedione
Platinum(II) complex
Cell apoptosis
Akt
GSK3β

ABSTRACT

A new platinum(II) complex, [Pt(ClClQ)(DMSO)Cl] (**1**), utilizing 6,7-dichloro-5,8-quinolinedione (ClClQ) as a ligand, has been synthesized and fully characterized. Single-crystal X-ray diffraction and other spectroscopic and analytical methods revealed that the coordination geometry of Pt(II) in complex **1** can also be described as a four-coordinated square planar geometry. The aim of the study was to explore the *in vitro* anticancer properties of complex **1**. Our studies showed that complex **1** can regulate the viability of testicular seminoma cells *in vitro*, including cell proliferation and apoptosis. We further observed negative regulation by complex **1** of the expression levels of the key elements in the phosphoinositide-3 kinase (PI3K)/protein kinase B (Akt)/glycogen synthase kinase-3β (GSK3β) pathway, including phosphorylated phosphoinositide-3 kinase (p-PI3K), phosphorylated protein kinase B(p-Akt) and phosphorylated glycogen synthase kinase-3β (p-GSK3β). Moreover, the negative effect of complex **1** was reversed by LiCl, a GSK3β-specific inhibitor of the PI3K signaling pathway. Meanwhile, the levels of Bcl2 associated death promoter (Bad), cytochrome *c*, active-caspase-3 and active-caspase-9 increased significantly. In conclusion, we observed that complex **1** can regulate the viability of testicular seminoma cells through the PI3K/Akt/GSK3β signaling pathway and the mitochondria-mediated apoptotic pathway *in vitro*, and thus, complex **1** may have potential for use as a drug in the treatment of testicular germ cell tumors.

1. Introduction

Platinum-based anticancer drugs, such as cisplatin and carboplatin, have proven to be highly successful in the area of anticancer chemistry, stimulating the development of new drugs that utilize this metal host [1]. Testicular seminoma is the most commonly occurring solid tumor type in males [2,3]. Furthermore, the standard first-line cisplatin-based chemotherapy regimens are the most common therapy for testicular seminoma in clinical practice [4–6]. However, platinum-based drugs lead to severe side effects during the course of treatment, which has motivated chemists to find new metal-based anticancer drugs [7]. Cisplatin has been reported to possess anticancer activity by inducing apoptosis in cancer cells [8,9]. Therefore, the design and development of novel drugs with the ability to trigger apoptosis is now considered the most promising strategy for the discovery of new anticancer drugs for use in the treatment of testicular seminoma [10–12].

Quinoline and its derivatives have attracted the attention of both synthetic and biological chemists on account of the diversity of their chemical and pharmacological properties [13,14]. The suite of quinoline derivatives possesses a wide range of biological activities, such as antibacterial properties, anti-inflammatory functions, anticancer activities, *etc.* [15–20] The 5,8-quinolinedione moiety was shown to exhibit cytotoxic activity against cancer cell lines such as melanoma and breast cancer cells. Thus, the anticancer activities of 5,8-quinolinedione have attracted significant attention in recent years [21]. A series of quinoline-derived transition metal complexes, such as quilamine-iron chelators, clioquinol copper(II) and zinc(II) complexes, copper(II) and iron (II) complexes and ruthenium(II) complexes, were shown to possess good anticancer ability [22–26]. The anticancer mechanism of the quinoline derivatives is possibly due to their action as a

* Corresponding author.
E-mail address: mmcct@126.com (Y. Tang).

https://doi.org/10.1016/j.jinorgbio.2019.110701
Received 25 January 2019; Received in revised form 25 April 2019; Accepted 25 April 2019
Available online 27 April 2019

phosphoinositide-3 kinase (PI3K)/protein kinase B (Akt) inhibitor, mammalian target of rapamycin (mTOR) inhibitor, vascular endothelial growth factor receptor 2(VEGFR-2) inhibitor, cellular-mesenchymal to epithelial transition factor (c-Met) inhibitor, *etc.* [27–29]

The PI3K/Akt pathway is one of the crucial signaling cascades in humans. This pathway participates in many physiologic processes, such as cell survival, proliferation and apoptosis [30,31]. Several studies have reported the abnormal activation of this signaling pathway relative to the formation of seminoma [32,33]. However, few studies have explored the application of platinum-based agents with quinoline derivatives in the treatment of testicular seminomas.

Therefore, we synthesized a new platinum(II) complex, [Pt(ClClQ)(DMSO)Cl] (**1**), utilizing 6,7-dichloro-5,8-quinolinedione (ClClQ) as a ligand. The biological activity and action mechanism of complex **1**, such as its cytotoxicity, cell cycle and cell apoptosis, were studied.

2. Results and discussion

2.1. Synthesis

5-Nitroso-8-hydroxyquinoline hydrochloride and 5-amino-8-hydroxyquinoline sulfate were synthesized according to reported procedures [34]. In addition, the synthesis procedures of [Pt(ClClQ)(DMSO)Cl] (**1**) are shown in Scheme 1. Complex **1** was obtained by the reaction of the 6,7-dichloro-5,8-quinolinedione (ClClQ) ligand and *cis*-$Pt(DMSO)_2Cl_2$ in a 1:1 ratio in CH_3OH and acetone (v:v = 20 mL:1 mL) and in CH_3OH and DMSO (v:v = 20 mL:1 mL) under refluxing (Scheme 1). The 6,7-dichloro-5,8-quinolinedione ligand and Pt(II) complex **1** were characterized by IR, ^1H and ^{13}C NMR spectrometry, electrospray ionization mass spectrometry (ESI-MS), single-crystal X-ray diffraction analyses and elemental analyses (Figs. S1–S6).

2.2. Crystal structures

The molecular structure of complex **1** is illustrated in Fig. 1. The detailed crystallographic data and structural refinement parameters are summarized in Table 1. Selected bond lengths and bond angles are listed in Tables 2 − 3. From Fig. 1, it can be seen that in each case, the Pt(II) center is four-coordinated by the chelating ClClQ ligand (N^O-ClClQ) *via* the O atom and heterocyclic nitrogen (N) atom, one DMSO ligand *via* the S atom, and one Cl atom, to form a square-planar geometry. The bite angles of the chelate rings (N(1)–Pt(1)–Cl(1), N(1)–Pt(1)–S(1) and N(1)–Pt(1)–O(1)) were 170.20(18), 100.66(18) and 80.7(2)°, respectively. The bond lengths of Pt−O (2.057(5)Å) and Pt−N (2.041(6)Å) were significantly shorter than those of Pt−Cl (2.286(2)Å) and Pt−S (2.2120(18)Å), which fell within the normal range.

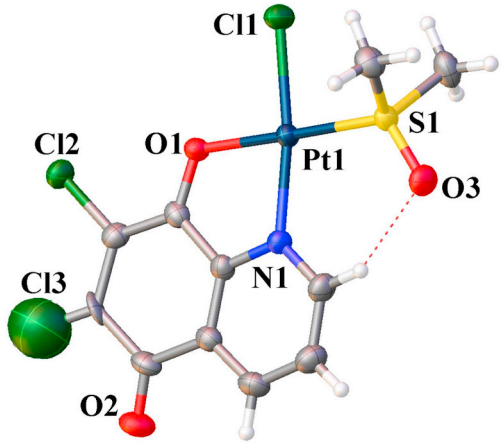

Fig. 1. ORTEP view of the molecular structures and atomic labeling of complex **1**.

Table 1
Crystal data and structure refinement details for complex **1**.

Empirical formula	$C_{11}H_9Cl_3NO_3PtS$
Formula weight	536.69
Temperature/K	296.15
Crystal system	Monoclinic
Space group	$P2_1/c$
a/Å	11.9240(2)
b/Å	13.4714(2)
c/Å	8.8326(2)
α/°	90
β/°	103.974(2)
γ/°	90
Volume/Å^3	1376.82(5)
Z	4
ρ_{calc}g/cm^3	2.589
μ/mm^{-1}	10.928
F(000)	1004.0
Crystal size/mm^3	0.22 × 0.2 × 0.18
Radiation	MoKα (λ = 0.71073)
2Θ range for data collection/°	7 to 52.728
Index ranges	−14 ≤ h ≤ 14, −16 ≤ k ≤ 15, −11 ≤ l ≤ 10
Reflections collected	9140
Independent reflections	2807 [R_{int} = 0.0268, R_{sigma} = 0.0298]
Data/restraints/parameters	2807/0/183
Goodness-of-fit on F^2	1.053
Final R indexes [$I \geq 2\sigma$ (I)]	R_1 = 0.0324, wR_2 = 0.0835
Final R indexes [all data]	R_1 = 0.0395, wR_2 = 0.0881
Largest diff. peak/hole/e Å^{-3}	1.59/−1.92

[a]$R_1 = \Sigma||F_o| - |F_c||/\Sigma|F_o|$; [b]$wR_2 = [\Sigma w(F_o^2 - F_c^2)^2/\Sigma w(F_o^2)^2]^{1/2}$.

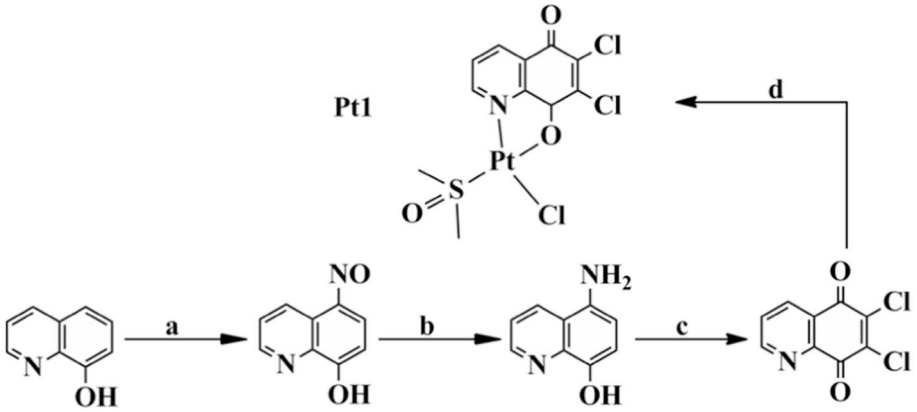

Scheme 1. Synthetic routes for the preparation of 6,7-dichloro-5,8-quinolinedione and complex **1**. Reagents and solvents are the following: (a) $NaNO_2$ (30 g), concentrated HCl (37.0 mL), H_2O (150.0 mL), 4 °C, 1 h; (b) 5 M NaOH solution (269.0 mL), H_2O (160.0 mL), $Na_2S_2O_4$ (95.0 g), 80 °C, 2 h; 6.0 M H_2SO_4 (250 mL), 2 h; (c) $KClO_3$ (5.5 g), concentrated HCl (69.0 mL), 60 °C, 30 min; (d) CH_3OH and acetone (v:v = 20 mL:1 mL), refluxing, 24 h.

Table 2
Selected bond lengths (Å) for complex **1**.

Atom	Atom	Length/Å	Atom	Atom	Length/Å
Pt01	S1	2.2120(18)	Cl3	C8	1.234(9)
Pt01	Cl1	2.286(2)	C11	C10	1.478(10)
Pt01	O2	2.057(5)	C11	C6	1.382(10)
Pt01	N1	2.041(6)	C10	C9	1.374(11)
S1	O1	1.465(6)	O3	C7	1.196(10)
S1	C2	1.775(8)	C3	C4	1.376(12)
S1	C1	1.775(8)	C9	C8	1.441(11)
Cl2	C9	1.728(8)	C6	C7	1.487(11)
O2	C10	1.299(9)	C6	C5	1.371(12)
N1	C11	1.358(9)	C8	C7	1.500(12)
N1	C3	1.345(10)	C4	C5	1.390(12)

Table 3
Selected bond angles (°) for complex **1**.

Atom	Atom	Atom	Angle/°	Atom	Atom	Atom	Angle/°
S1	Pt01	Cl1	89.13(7)	O2	C10	C11	117.3(6)
O2	Pt01	S1	178.35(15)	O2	C10	C9	123.8(7)
O2	Pt01	Cl1	89.54(15)	C9	C10	C11	118.9(7)
N1	Pt01	S1	100.66(18)	N1	C3	C4	122.9(8)
N1	Pt01	Cl1	170.20(18)	C10	C9	Cl2	119.8(6)
N1	Pt01	O2	80.7(2)	C10	C9	C8	122.1(7)
O1	S1	Pt01	117.0(3)	C8	C9	Cl2	118.1(6)
O1	S1	C2	107.9(4)	C11	C6	C7	119.3(7)
O1	S1	C1	107.5(4)	C5	C6	C11	118.8(7)
C2	S1	Pt01	110.1(3)	C5	C6	C7	121.9(7)
C2	S1	C1	103.3(4)	Cl3	C8	C9	123.1(8)
C1	S1	Pt01	110.3(3)	Cl3	C8	C7	117.6(7)
C10	O2	Pt01	113.7(5)	C9	C8	C7	119.3(6)
C11	N1	Pt01	113.1(5)	O3	C7	C6	121.3(8)
C3	N1	Pt01	128.9(5)	O3	C7	C8	121.6(7)
C3	N1	C11	118.0(6)	C6	C7	C8	117.1(6)
N1	C11	C10	115.2(6)	C3	C4	C5	118.2(8)
N1	C11	C6	122.2(7)	C6	C5	C4	119.9(7)
C6	C11	C10	122.7(7)				

2.3. Complex 1 modulated the viability and invasive ability of testicular seminoma cells

The cytotoxicity of complex **1** against the testicular seminoma TCam-2 cells and SEM-1 cells was tested by 3-(4,5-dimethylthiazol-2-yl)-2,5-diphenyltetrazolium bromide (MTT) assays. The concentration of DMSO is approximately 0.1% after calculation, thus 0.1% concentration of DMSO was used as a vehicle control. As demonstrated in Fig. 2, after incubation with different concentrations of complex **1** for 0, 24, 48, and 72 h, both cell lines presented a time-dependent and a dose-dependent inhibition of cell viability. The *in vitro* antitumor activity of complex **1** was further quantified by determining its corresponding half maximal inhibitory concentration (IC50) levels. The effect of 0.1% concentration of DMSO on cells was negligible. As shown in Table 4, the IC50 values for complex **1** against TCam-2 cells and SEM-1 cells were 9.53 ± 0.43 μM and 8.89 ± 0.47 μM, respectively, which exhibited higher cytotoxicity against cisplatin. The impact of complex **1** on tumor cell invasion was tested by cell invasion assays at 48 h. Compared with untreated cells, the viability and invasive ability of the tumor cells were significantly weakened after incubation with complex **1** in both testicular seminoma cell lines (Figs. 2 and 3).

2.4. Complex 1 regulates the cell cycle transition of seminoma cells

Complex **1** was found to reduce the cell proliferation results based on the slower progression of cells through the cell cycle. To evaluate these mechanisms, we first investigated the cell cycle distribution changes under different treatments. Glycogen synthase kinase-3β (GSK3β) is involved in the regulation of cellular differentiation, proliferation and apoptosis of cancer cells by certain signaling pathways [35,36]. Herein, through a series of experiments, we utilized the GSK3β inhibitor, LiCl, as a reference drug to clarify whether GSK3β was involved in the antitumor mechanism of complex **1** [37]. As shown in Fig. 4, the cytometric profiles of the TCam-2 cells and SEM-1 cells treated with Complex **1** for 48 h indicated that the respective S phase populations were 16.55% and 17.22%. Compared with the untreated cells, their respective S phase populations were 13.56% and 11.91% lower than that of the untreated cells, respectively. The data showed that complex **1** induces cell cycle arrest in G0/G1 phase in both cell lines with a lower proliferation index, while the GSK3β specific inhibitor accelerates cell cycle progression by promoting the transition from G0/G1 phase to S phase. These results suggested that complex **1** significantly arrested the cell cycle in G0/G1 phase in the seminomas. In addition, GSK3β, which is a downstream target of the PI3K/Akt signaling pathway, may be involved in the antitumor mechanism of complex **1**.

2.5. Complex 1 promotes apoptosis of seminoma cells

Cell cycle arrest and cell apoptosis induction were considered to be closely correlated in tumor cells, and thus, we next chose to examine cell apoptosis in the testicular seminoma cells as induced by complex **1** by flow cytometry. As shown in Fig. 5, compared with that in the control group, complex **1** significantly induced apoptosis in both testicular seminoma cell lines. The significant increase in the percentages of apoptotic cells and early apoptotic cells strongly suggested that complex **1** could effectively induce apoptosis in seminoma cells. Interestingly, LiCl was able to decrease the ability of complex **1** to induce cell apoptosis.

2.6. Complex 1 exhibits antitumor activity through the PI3K/Akt/GSK3β signaling pathway in seminoma cells

Our previous study indicates that the development and migration of seminoma cells *via* regulation of the PI3K/Akt signaling pathway [38,39]. Akt is a crucial component in PI3K signaling and has the ability to regulate downstream targets, such as mTOR and GSK3β, indicating that Akt is involved in many important physiologic processes [40]. Therefore, based on the previous results, we employed Western blotting (WB) to explore whether PI3K/Akt/GSK3β signaling was involved in the complex **1** antitumor mechanism with regard to testicular seminoma. GSK-3β played a crucial role in negative expression of cyclin D1 *via* phosphorylation of cyclin D1, and phosphorylation of GSK-3β was the inactivated form of GSK-3β. However, LiCl could promote the phosphorylation of GSK-3β, which has positive modulation on expression of cyclin D1. As shown in Fig. 6, we found that the expression levels of phosphorylated PI3K, Akt and GSK-3β in TCam-2 cells and SEM-1 cells were decreased after complex **1** treatment for 48 h, while there were not significant changes in PI3K or AKT. As expected, the expression levels of cyclin D1 were inhibited in two seminoma cells. It has previously been reported that cyclin D1 is an up-regulator to cell cycle progression and drives the G1/S phase transition. Compared with merely complex **1** treatment groups, the expression levels of phosphorylated GSK-3β and cyclin D1 were significantly increased in complex **1** plus LiCl treatment for 48 h, while the expression levels of phosphorylated PI3K and Akt just had a mild increase. These results suggested that the PI3K/Akt/GSK3β signaling pathway might be involved in the antitumor mechanism of complex **1** in seminoma cells.

2.7. Mitochondria-mediated apoptotic pathway is involved in complex 1 antitumor mechanism

The mitochondria-associated apoptotic pathway is one of the major apoptosis pathways and participates in the cellular response of tumors to many anticancer drugs [41]. To determine whether the

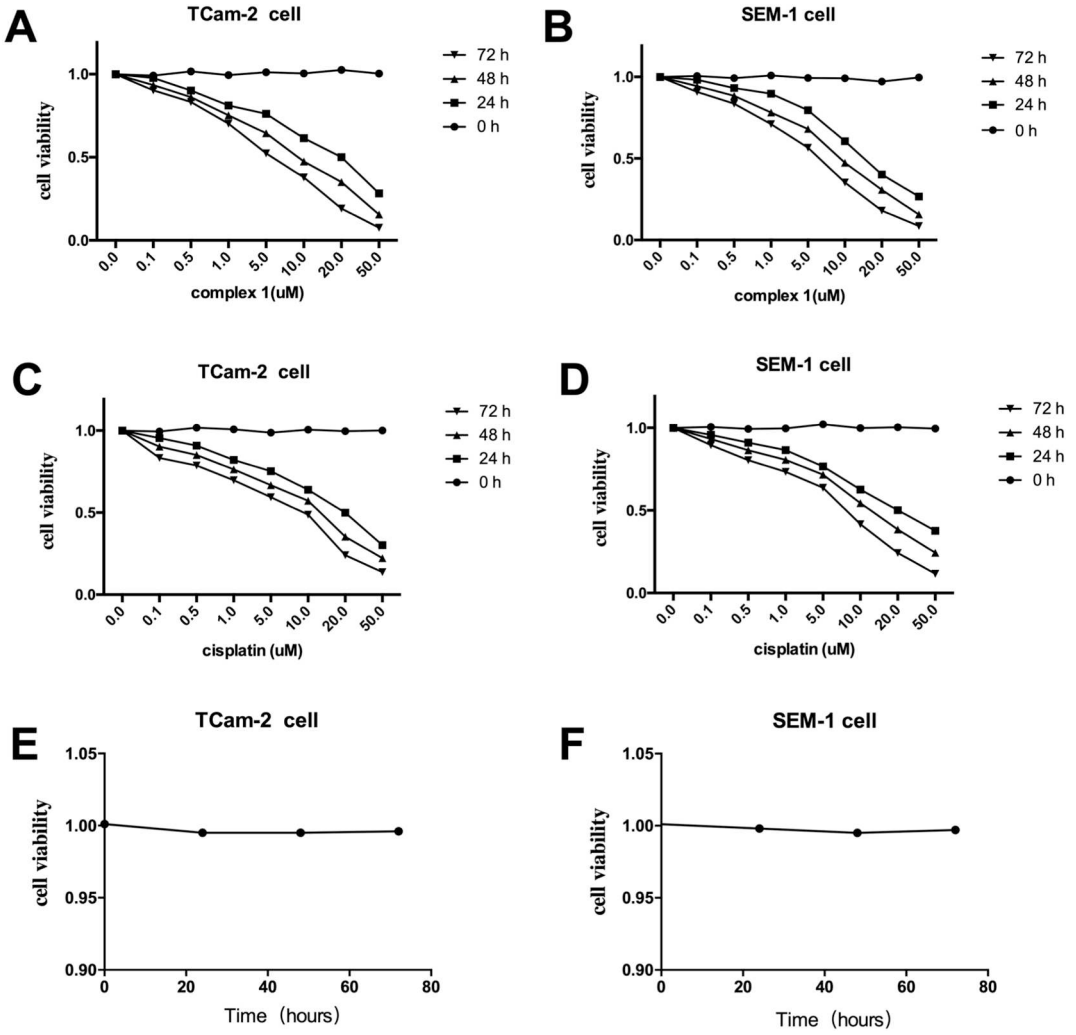

Fig. 2. The cytotoxicity of complex **1** against testicular seminoma TCam-2 cells and SEM-1 cells. (A and C) Viability of TCam-2 cells after incubation with different concentrations of complex **1** and cisplatin for 0, 24, 48, and 72 h. (B and D) Viability of SEM-1 cells after incubation with different concentrations of complex **1** and cisplatin for 0, 24, 48, and 72 h. (E and F) Viability of TCam-2 cells and SEM-1 cells after incubation with 0.1% concentration of DMSO for 0, 24, 48, and 72 h.

Table 4
IC50 (μM) values of complex **1** on testicular seminoma cells for 48 h.

Compounds	IC50 (μM)	
	TCam-2 cells	SEM-1 cells
Complex **1**	9.53 ± 0.43	8.89 ± 0.47
Cisplatin	14.73 ± 0.37	12.38 ± 0.41

mitochondria-associated apoptotic pathway is involved in the anti-tumor activity of complex **1** in seminoma cells, we performed an analysis of pro-apoptotic proteins (Bcl2 associated death promoter (Bad), cytochrome *c*) [42]. Moreover, it is also believed that the activation of caspase-9 and caspase-3 stimulates mitochondrial cell death signals; thus, we also investigated the changes in the expression levels of these two proteins. In Fig. 6, compared to the control cells, the WB results showed a significant increase in Bad, cytochrome *c*, caspase-9 ratio (activated/total) and caspase-3 ratio (activated/total) levels after

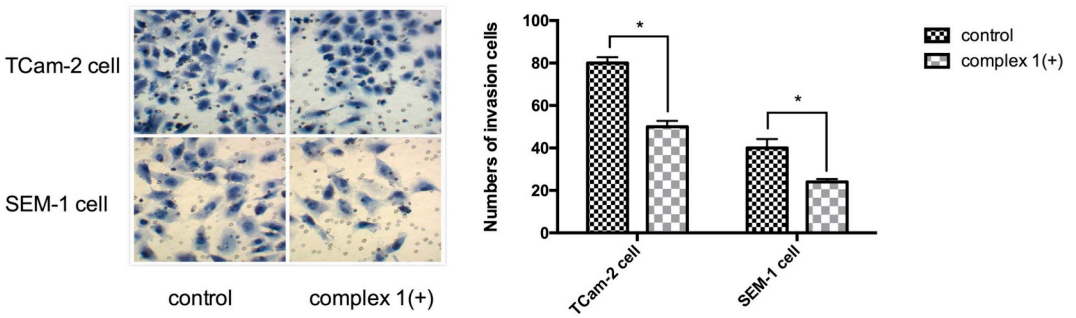

Fig. 3. The invasive ability of the testicular seminoma TCam-2 cells and SEM-1 cells after incubation with complex **1** (1 μM) for 24 h. Control group means no drug treatment, complex (+) group means treatment with complex **1**. *$p < 0.05$ compared to negative control values.

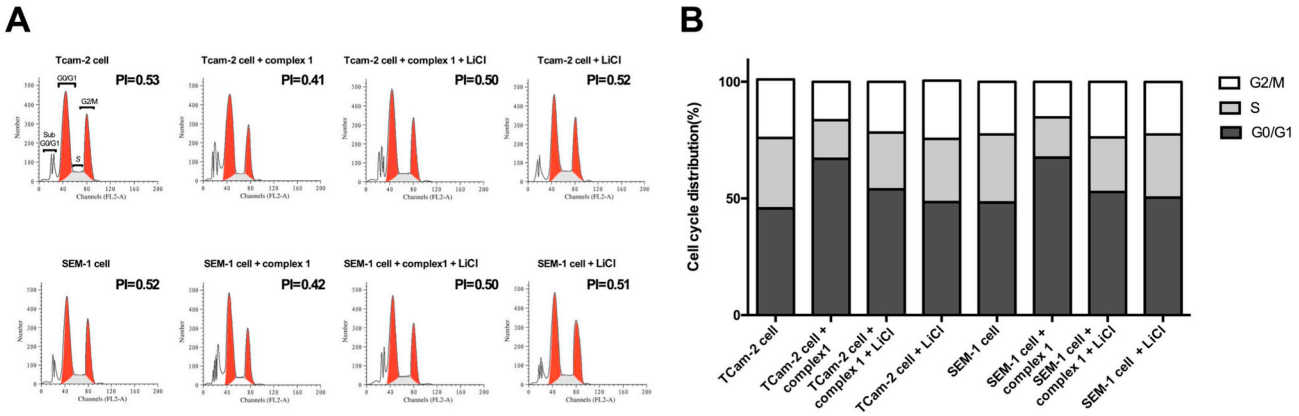

Fig. 4. Complex **1** regulates the cell cycle transition of seminoma cells. (A) Cell cycle distribution in seminoma TCam-2 cells and SEM-1 cells following complex 1 (10 μM) treatment for 48 h was analyzed by flow cytometry. (B) Quantitative summary of the cell cycle distribution in different groups.

complex **1** treatment in TCam-2 cells and SEM-1 cells for 48 h. It has been reported that Akt negatively regulated the expression of caspase-9 and caspase-3. However, as shown in WB results, there were significant decrease in caspase-9 and caspase-3, and no significant changes in Akt, which indicates that lower expression of caspase-9 and caspase-3 was not relevant to the Akt. These observations suggested that apoptosis, when exposed to complex **1**, could be attributed to the mitochondria-mediated apoptotic pathway in seminoma cells.

3. Conclusions

A new platinum complex, known as complex **1** and utilizing the 6,7-dichloro-5,8-quinolinedione ligand, was synthesized and fully characterized. This complex exhibited significant antitumor activity and cytotoxicity against human seminoma cells. In detail, complex **1** could weaken the viability and invasive ability of tumor cells. Moreover, complex **1** induces testicular seminoma cell cycle arrest in the G0/G1 phase. The molecular mechanisms of the antitumor activity of complex **1** include its ability to induce tumor cell apoptosis through the PI3K/Akt signaling pathway and the mitochondria-mediated apoptotic pathway. This complex may serve as a potential drug in the treatment of testicular germ cell tumors.

4. Experimental methods

4.1. Synthesis

4.1.1. Synthesis of 6,7-dichloro-5,8-quinolinedione

5-Nitroso-8-hydroxyquinoline hydrochloride and 5-amino-8-hydroxyquinoline sulfate were synthesized according to the reported procedures. Consequently, $KClO_3$ (5.5 g) was added to a mixture of 5-amino-8-hydroxyquinoline sulfate (9.0 g, 0.35 mol) in concentrated HCl (69.0 mL) at 60 °C for 30 min. The mixture was poured into ice water (500 mL). The yellow 6,7-dichloro-5,8-quinolinedione product was prepared in methanol/CHCl3 (v:v = 100:1) under solvothermal conditions and suitable for structural characterization. Yield (7.5 g, 90.0%). ESI-MS *m/z*: 360.2 $[M + DMSO + CH_3CN + H]^+$. ^1H NMR (400 MHz, DMSO-d_6) δ 9.05 (dd, J = 4.7, 1.7 Hz, 1H), 8.46 (dd, J = 7.9, 1.7 Hz, 1H), 7.89 (dd, J = 7.9, 4.7 Hz, 1H). ^{13}C NMR (100 MHz, DMSO-d_6) δ 176.8, 174.7, 154.9, 147.5, 143.6, 142.1, 135.4, 129.0, 128.8. IR (KBr): 3367, 1693, 1680, 1573, 1559, 1288, 1198, 1140, 896, 826, 725, 695, 637, 478 cm^{-1}. Elemental analysis calculated (%) for $C_9H_3Cl_2NO_2$: C 47.40, H 1.33, N 6.14; found: C 47.43, H 1.38, N 6.10.

4.1.2. Synthesis of complex *1*

Complex **1** was prepared by treating cis-$Pt(DMSO)_2Cl_2$ (0.0422 g, 0.1 mmol) with 6,7-dichloro-5,8-quinolinedione (0.0227 g, 0.1 mmol)

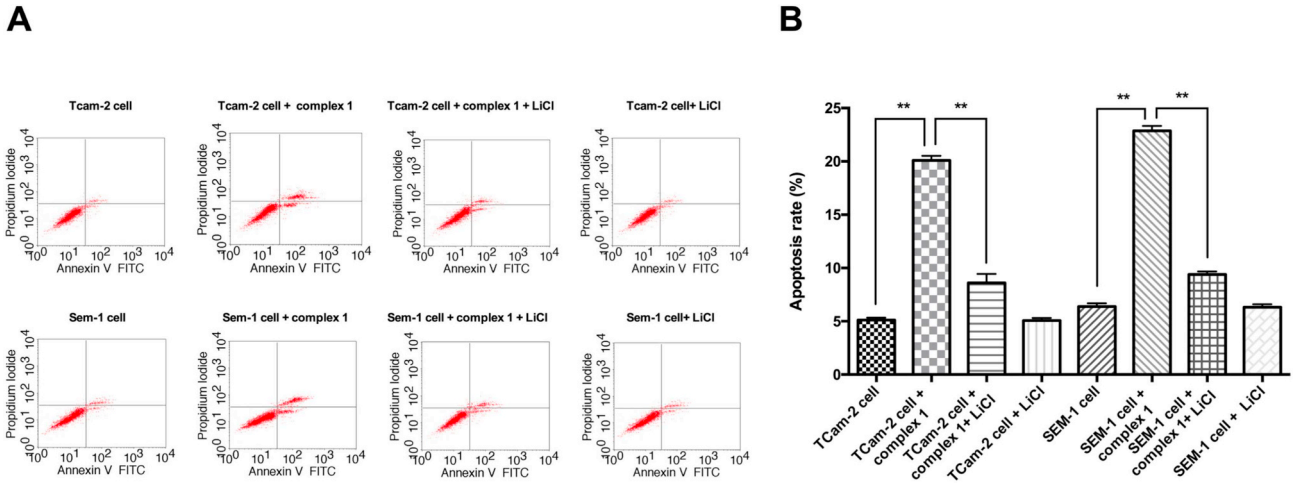

Fig. 5. The effect of complex **1** on early cell apoptosis. (A) Cells were treated with complex **1** (1 μM) followed by staining with Annexin V-fluorescein isothiocyanate and propidium iodide and then were analyzed by flow cytometry. (B) Quantitative summary of early apoptosis rate in different groups. Complex **1** was able to significantly induce apoptosis in both testicular seminoma cell lines. LiCl decreased the apoptosis rate after cells were treated with complex **1**. Compared as indicated, $^{**}p < 0.01$.

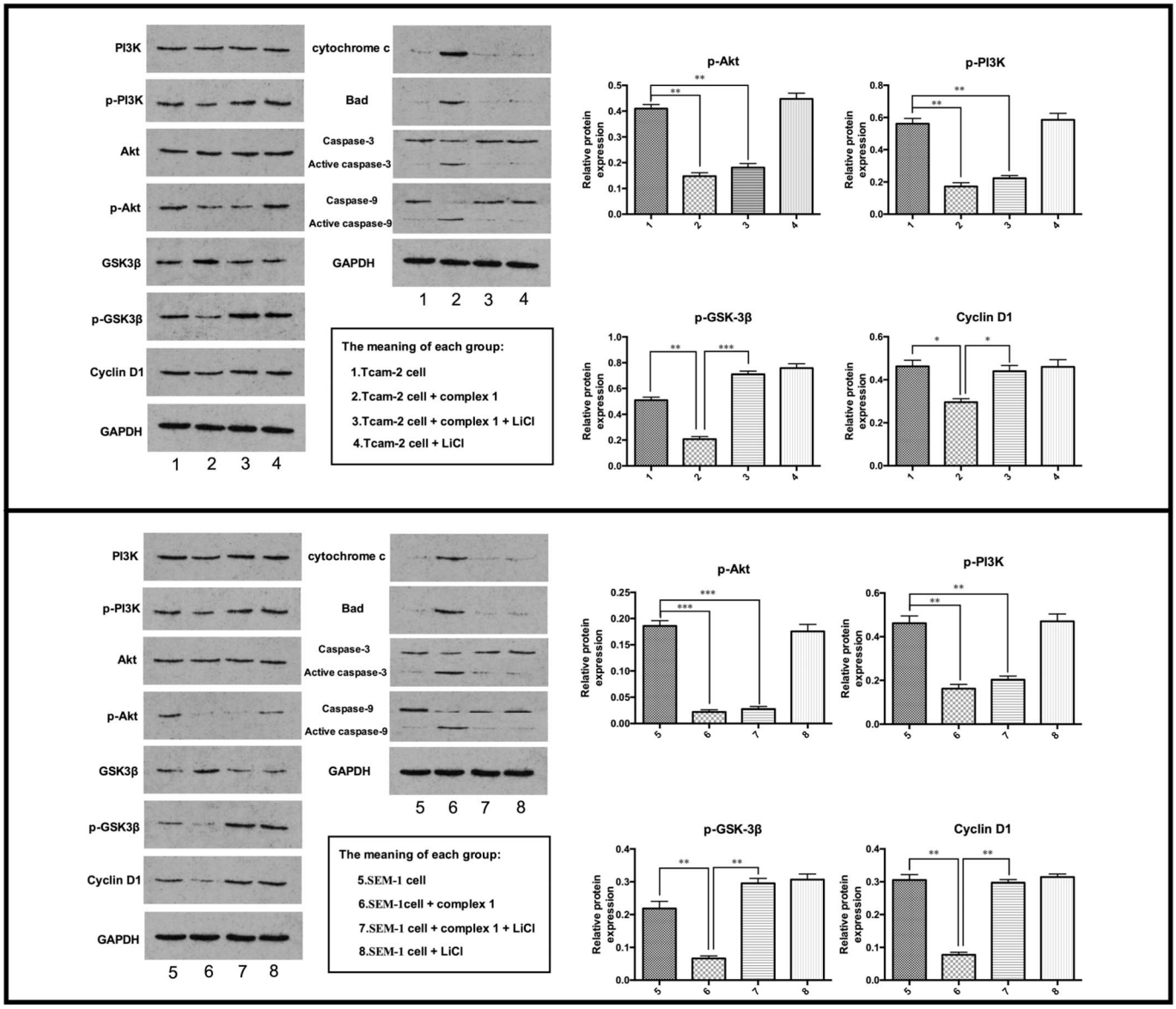

Fig. 6. Protein expression of PI3K, p-PI3K, Akt, p-Akt, GSK-3β, p-GSK-3β and cyclin D1 was measured by protein gel blotting. Glyceraldehyde-3-phosphate dehydrogenase (GAPDH) served as the internal control. The expression levels of phosphorylated PI3K, Akt and GSK-3β and cyclin D1 in TCam-2 cells and SEM-1 cells decreased after complex **1** treatment for 48 h. Moreover, the expression levels of Bad, cytochrome *c*, active-caspase-9 and active-caspase-3 were significantly increased. *p < 0.05, **p < 0.01, ***p < 0.001.

in CH_3OH and acetone (v:v = 20 mL:1 mL) under refluxing. And the resulting brown product suitable for structural characterization were isolated, washed with ethanol and ether, and air-dried, respectively. Yield (0.0459 g, 85.69%). IR (KBr): 3405, 3082, 3023, 2931, 1711, 1650, 1611, 1539, 1465, 1367, 1301, 1170, 1136, 1024, 854, 691, 654, 632, 537, 452 cm^{-1}. ^{13}C NMR (126 MHz, DMSO) δ 175.03, 173.05, 170.71, 158.44, 151.69, 138.30, 137.52, 128.11, 40.92. ^{1}H NMR (500 MHz, DMSO-d_6) ¦Ä 9.42 (dd, J = 6.1, 1.3 Hz, 1H), 8.59 ¨C 8.54 (m, 1H), 7.95 (m, J = 7.8, 5.4 Hz, 1H), 2.54(s,6H). Elemental analysis calculated (%) for $C_{11}H_{10}Cl_3NO_3PtS$: C 24.57, H 1.87, N 2.60; found: C 24.62, H 1.90, N 2.57.

4.2. Materials and methods for X-ray crystallography

Single-crystal X-ray crystallography of complex **1** was performed using a SuperNova CCD diffractometer equipped with graphite monochromated Mo Kα radiation (λ = 0.710 73 Å) at room temperature. The structures were solved with direct methods and refined using SHELX-97 programs. The nonhydrogen atoms were located using successive difference Fourier synthesis. The final refinement was performed using the full-matrix least-squares methods with anisotropic thermal parameters for no-hydrogen atoms on F_2. The hydrogen atoms were added theoretically to the atoms of concern. The parameters used intensity collection, and the associated refinements are summarized in Tables 1 – 3 together with the crystal data. The crystallographic data of complex **1** is available free of charge from The Cambridge Crystallographic Data Centre: CCDC 1839014.

4.3. Chemical compounds and antibodies

LiCl (Sigma-Aldrich, St. Louis, MO, USA) stock solution was prepared in water and then was sterilized and added to culture medium until a final concentration of 20 mM. Antibodies against PI3K (the p85 subunit, 1:8000), p-PI3K (Tyr607 of the p85 subunit, 1:8000), p-Akt (Ser473, 1:4000), cytochrome *c* (1:200) and caspase-3 (1:200) were obtained from Abcam Biotechnology (Cambridge, UK); antibodies

against caspase-9 (1:150) and GAPDH (1:8000) were purchased from Santa Cruz Biotechnology (Santa Cruz, CA, USA). Akt (1:600) and antibodies were purchased from Signalway Antibody Biotechnology (Baltimore, MD, USA), Cell Signaling Technology (Boston, MA, USA), Acris Biotechnology (San Diego, CA, USA) and Gen-eTex (Irvine, CA, USA), respectively.

4.4. Cell culture and treatment

The tumor cell lines TCam-2 cells and SEM-1 were kindly gifted from Dr. Riko Kitazawa (Department of Diagnostic Pathology, Ehime University Hospital, Matsuyama, Japan). All cell lines were maintained in complete medium (Roswell Park Memorial Institute Medium-1640 with 10% fetal calf serum, 2 mM L-glutamine, 100 U/mL penicillin, and 100 μg/mL streptomycin) in a humidified 5% CO_2, 37 °C incubator. A stock solution of complex **1** dissolved in DMSO at a concentration of 2.0 mM was prepared. The stock was diluted by phosphate buffer saline (PBS) to the required concentration immediately before use.

4.5. Cell viability assay

The cytotoxicity of complex 1 against the testicular seminoma cell lines TCam-2 and SEM-1 was measured by MTT assay. Cells were seeded at a density of 104 cells/well in 96-well plates for 24 h. For time-dependent and dose-dependent assays, the testicular seminoma TCam-2 and SEM-1 cell lines were treated with different concentrations (0 μM, 0.1 μM, 0.5 μM, 1.0 μM, 5 μM, 10 μM, 20 μM, and 50 μM) of complex 1 for 0 h, 24 h, 48 h, and 72 h. Then, the cells were incubated with 20 mL of MTT solution (5 mg/mL, Sigma-Aldrich) for 4 h at 37 °C. At different time points (0, 24, 48, 72 h), MTT was added as described above. Then, DMSO was added to each well to dissolve the purple-blue formazan crystals by gentle agitation. For each well, the absorbance at 570 nm (A570) was estimated using a Microplate Reader, with DMSO used as the blank.

4.6. Cell invasion assay

A cell invasion assay was performed using Transwell chambers with 8-μm pore inserts. Cell suspensions were seeded in the upper chamber, and 500 μL of Dulbecco's Modified Eagle's Medium containing fetal bovine serum was added to the lower chamber. The noninvading cells were removed with a cotton-tipped swab after 24 h of incubation, and the invading cells on the bottom surface of the membrane were stained with 0.1% crystal violet. The invading cells were quantified by counting ten random fields at ×200 magnification.

4.7. Cell apoptosis analysis

Apoptosis was assessed with an Annexin V- fluorescein isothiocyanate (FITC)/propidium iodide (PI) Apoptosis Detection Kit (Beyotime Institute of Biotechnology, Shanghai, People's Republic of China) according to the manufacturer's instructions. Briefly, after complex 1 treatment and incubation for 48 h, cells were collected, washed with PBS and labeled with Annexin V and propidium iodide in the dark using an Annexin V-FITC apoptosis detection kit (Beyotime Biotechnology, Shanghai, China). Cell apoptosis was subsequently analyzed by a FACSCalibur flow cytometry (BD Biosciences, San Jose, CA, USA).

4.8. Cell cycle analysis by flow cytometry

Cell cycle analysis was performed using the PI single staining method as described previously [43]. Briefly, two cell lines were incubated in 10% fatal bovine serun (FBS)-supplemented culture medium with complex 1 (10 μM) for 48 h at 37 °C and 5% CO_2. Then, cells were collected, washed and centrifuged at 1000 rpm and finally were fixed with 75% cold ethanol at 4 °C overnight. After staining in phosphatidylinositol (PtdIns) and ribonuclease (RNase) A at room temperature for 30 min in the dark, the percentage of cells in each cell cycle phase was determined with Cell Quest software and ModiFit (Verity Software House, Topsham, USA) by using a flow cytometer (BD Biosciences).

4.9. Western blotting

Western blotting (WB) was implemented as described previously [43]. Briefly, the cells were lysed in lysis buffer containing protease inhibitors. The protein concentration of lysates was determined by the bicinchoninic acid assay (Beyotime Biotechnology). Equal amounts of protein (20 mg) were separated by 10% sodium dodecylsulphate-polyacrylamide gel electrophoresis (SDS-PAGE) electrophoresis and subsequently transferred onto poly vinylidene fluoride (PVDF) membranes. Semi dry transfer was done in the WB protocol. The membranes were blocked with 5% non-fat dry milk in 0.2% Tween-20 in Tris-buffered saline (TBS-T) for 1 h at room temperature and then were probed with primary antibodies. Immunoreactivity was detected after incubation with a horseradish peroxidase-conjugated secondary antibody by the enhanced chemiluminescence method according to the instructions (Thermo Scientific, Waltham, MA, USA). GAPDH was stained as a loading control. The positive bands were analyzed by Gel-pro analyzer software, and the value of integrated optical density (IOD) was measured.

4.10. Data processing

The data are expressed as the mean ± standard deviation. A statistical analysis of the data was performed using SPSS 17.0 (SPSS Inc., Chicago, IL, USA). Statistical significance was determined using an analysis of variance followed by Student's *t*-tests. A value of $p < 0.05$ was considered to indicate a statistically significant difference.

Abbreviation

PBS	phosphate buffer saline
MTT	3-(4,5-dimethylthiazol-2-yl)-2,5-diphenyltetrazolium bromide
IC50	half maximal inhibitory concentration
TCam-2 cells	human testicular seminoma cell line
SEM-1 cells	human testicular seminoma cell line
FITC	fluorescein isothiocyanate
PI	propidium iodide

Disclosure of potential conflicts of interest

No potential conflicts of interest were disclosed.

Funding

This research was funded by the National Nature Science Foundation of China (81372181, J. Yang; 81571432, Y. Tang).

Acknowledgments

The authors thank Mr. Xiaohua Li for technical support.

Appendix A. Supplementary data

Supplementary data to this article can be found online at https://doi.org/10.1016/j.jinorgbio.2019.110701.

References

[1] V. Milacic, D. Chen, L. Ronconi, K.R. Landis-Piwowar, D. Fregona, Q.P. Dou, Cancer Res. 66 (2006) 10478–10486.
[2] N. Ismaili, S. Naciri, S. Afqir, N. Mellas, I. Bekkouch, S. Elmajjaoui, O. Masbah, N. Othmani, A. Flechon, J. Droz, H. Errihani, Cases J. 1 (2008) 357.

[3] V.M. Chia, Y. Li, S.M. Quraishi, B.I. Graubard, J.D. Figueroa, J.P. Weber, S.J. Chanock, M.V. Rubertone, R.L. Erickson, K.A. McGlynn, Int. J. Androl. 33 (2010) 588–596.
[4] M. Juliachs, C. Munoz, C.A. Moutinho, A. Vidal, E. Condom, M. Esteller, M. Graupera, O. Casanovas, J.R. Germa, A. Villanueva, F. Vinals, Clin. Cancer Res. 20 (2014) 658–667.
[5] T. Kobayashi, T. Fujii, Y. Jo, K. Kinugawa, M. Fujisawa, J. Urol. 171 (2004) 1929–1933.
[6] C.M. Squillante, D.J. Vaughn, Urologic Oncology: Seminars and Original Investigations 33 (2015) 363–369.
[7] P. Giannatempo, T. Greco, L. Mariani, N. Nicolai, S. Tana, E. Fare, D. Raggi, L. Piva, M. Catanzaro, D. Biasoni, T. Torelli, S. Stagni, B. Avuzzi, M. Maffezzini, G. Landoni, F. De Braud, A.M. Gianni, G. Sonpavde, R. Salvioni, A. Necchi, Ann. Oncol. 26 (2015) 657–668.
[8] B.D. Chatterjee, A. Mitra, G.S. De, Platin. Met. Rev. 50 (2006) 2–12.
[9] E. Wong, C.M. Giandomenico, Chem. Rev. 99 (1999) 2451–2466.
[10] P.U. Maheswari, M.v.d. Ster, S. Smulders, S. Barends, G.P.v. Wezel, C. Massera, S. Roy, H.d. Dulk, P. Gamez, J. Reedijk, Inorg. Chem. 47 (2008) 3719–3727.
[11] Y. Jin, J.A. Cowan, J. Am. Chem. Soc. 127 (2005) 8408–8415.
[12] F. Mancin, P. Scrimin, P. Tecilla, U. Tonellato, Chem. Commun. (Camb.) (2005) 2540–2548.
[13] R.E. Swenson, T.J. Sowin, H.Q. Zhang, J. Org. Chem. 67 (2002) 9182–9185.
[14] S. Madapa, Z. Tusi, S. Batra, Curr. Org. Chem. 12 (2008) 1116–1183.
[15] S. Kumar, S. Bawa, H. Gupta, Mini-Rev. Med. Chem. 9 (2009) 1648–1654.
[16] X. Mao, X. Li, R. Sprangers, X. Wang, A. Venugopal, T. Wood, Y. Zhang, D.A. Kuntz, E. Coe, S. Trudel, D. Rose, R.A. Batey, L.E. Kay, A.D. Schimmer, Leukemia 23 (2009) 585–590.
[17] Z.F. Chen, Y.Q. Gu, X.Y. Song, Eur. J. Med. Chem. (2013) 194–202.
[18] Z.F. Chen, Y. Peng, Y.Q. Gu, Y.C. Liu, M. Liu, K.B. Huang, K. Hu, H. Liang, Eur. J. Med. Chem. 62 (2013) 51–58.
[19] Q.P. Qin, Z.F. Chen, J.L. Qin, X.J. He, Y.L. Li, Y.C. Liu, K.B. Huang, H. Liang, Eur. J. Med. Chem. 92 (2015) 302–313.
[20] X. Jia, F.F. Yang, J. Li, J.Y. Liu, J.P. Xue, J. Med. Chem. 56 (2013) 5797–5805.
[21] M. Kadela, M. Jastrzębska, E. Bębenek, E. Chrobak, M. Latocha, J. Kusz, M. Książek, S. Boryczka, Molecules 21 (2016) 156.
[22] V. Corce, S. Renaud, I. Cannie, K. Julienne, S.G. Gouin, O. Loreal, F. Gaboriau, D. Deniaud, Bioconjug. Chem. 25 (2014) 320–334.
[23] C.M. Santos, S. Cabrera, C. Ríos-Luci, Dalton Trans. 42 (2013) 13343–13348.
[24] L. Yang, J. Zhang, C. Wang, X. Qin, Q. Yu, Y. Zhou, J. Liu, Metallomics 6 (2014) 518–531.
[25] M. Gobec, J. Kljun, I. Sosic, I. Mlinaric-Rascan, M. Ursic, S. Gobec, I. Turel, Dalton Trans. 43 (2014) 9045–9051.
[26] Y.C. Liu, J.H. Wei, Z.F. Chen, M. Liu, Y.Q. Gu, K.B. Huang, Z.Q. Li, H. Liang, Eur. J. Med. Chem. 69 (2013) 554–563.
[27] R. Roskoski, Jr., Crit. Rev. Oncol. Hematol., vol. 62, 2007, pp. 179–213.
[28] Y. Wang, J. Ai, Y. Wang, Y. Chen, L. Wang, G. Liu, M. Geng, A. Zhang, J. Med. Chem. 54 (2011) 2127–2142.
[29] S.D. Knight, N.D. Adams, J.L. Burgess, A.M. Chaudhari, M.G. Darcy, C.A. Donatelli, J.I. Luengo, K.A. Newlander, C.A. Parrish, L.H. Ridgers, M.A. Sarpong, S.J. Schmidt, G.S. Van Aller, J.D. Carson, M.A. Diamond, P.A. Elkins, C.M. Gardiner, E. Garver, S.A. Gilbert, R.R. Gontarek, J.R. Jackson, K.L. Kershner, L. Luo, K. Raha, C.S. Sherk, C.M. Sung, D. Sutton, P.J. Tummino, R.J. Wegrzyn, K.R. Auger, D. Dhanak, ACS Med. Chem. Lett. 1 (2010) 39–43.
[30] L.C. Cantley, Science 296 (2002) 1655–1657.
[31] M.T. Boudewijn, P.J. Coffer, Nature 376 (1995) 599.
[32] Y. Nakai, N. Nonomura, D. Oka, M. Shiba, Y. Arai, M. Nakayama, H. Inoue, K. Nishimura, K. Aozasa, Y. Mizutani, T. Miki, A. Okuyama, Biochem. Biophys. Res. Commun. 337 (2005) 289–296.
[33] D.A. Altomare, J.R. Testa, Oncogene 24 (2005) 7455–7464.
[34] C.K. Ryu, H.J. Kim, Arch. Pharm. Res. 17 (1994) 139.
[35] M. Sharma, W.W. Chuang, Z. Sun, J. Biol. Chem. 277 (2002) 30935–30941.
[36] S. Attarha, A. Roy, B. Westermark, E. Tchougounova, Cell. Signal. 37 (2017) 81–92.
[37] Z.-Q. Fu, Y. Yang, J. Song, Q. Jiang, Z.-C. Liu, Q. Wang, L.-Q. Zhu, J.-Z. Wang, Q. Tian, J. Alzheimers Dis. 21 (2010) 1107–1117.
[38] X. Jiang, D. Li, J. Yang, J. Wen, H. Chen, X. Xiao, Y. Dai, J. Yang, Y. Tang, Tohoku J. Exp. Med. 225 (2011) 311–318.
[39] H. Chen, J. Sun, Y. He, Q. Zou, Q. Wu, Y. Tang, Tohoku J. Exp. Med. 235 (2015) 103–109.
[40] D. Sun, A. Sawada, M. Nakashima, T. Kobayashi, O. Ogawa, Y. Matsui, Urol. Oncol. 33 (2015) 111 e117–126.
[41] L. Yang, T. Shi, F. Liu, C. Ren, Z. Wang, Y. Li, X. Tu, G. Yang, X. Cheng, PLoS One 10 (2015) e0120334.
[42] D.W. Nicholson, N. A., Science 299 (2003) 214–215.
[43] Y. Wang, Y. Gan, Z. Tan, J. Zhou, R. Kitazawa, X. Jiang, Y. Tang, J. Yang, Onco Targets Ther 9 (2016) 409–420.